

Circulating miR-125b-5p and miR-99a-5p are associated with disease progression in pancreatic cancer patients after resection

Eveline E. Vietsch^{1,2}

Ivana Peran¹

Mustafa Suker²

Thierry P.P. van den Bosch³

Johan M. Kros³

Anton Wellstein¹

Casper H.J. van Eijck²

1 Department of Oncology, Lombardi Comprehensive Cancer Center, Georgetown University, Washington DC, USA

2 Department of Surgery, Erasmus Medical Center, Rotterdam, The Netherlands

3 Department of Pathology, Erasmus Medical Center, Rotterdam, The Netherlands

Submitted

ABSTRACT

Objectives: Monitoring responses to therapy using changes in the expression of circulating microRNAs (miRs) could be useful in prognostication of pancreatic cancer (PDAC) patients.

Methods: Changes in circulating miRs due to cancer progression in the transgenic *Kras*^{G12D/+}; *Trp53*^{R172H/+}; *P48-Cre* (KPC) animal model of PDAC were analyzed for serum miRs that are altered in metastatic disease. An analysis of serum miR expression profiles of human patients with resectable PDAC was performed using the novel RT-qPCR based IDEAL Assay which allows for highly sensitive and miR-specific quantitation. Up to 250 serum miRs from 28 patients with PDAC were analyzed for changes indicative of PDAC recurrence after resection.

Results: Consistent with the results in the KPC mice, we found that high serum miR-125b-5p and miR-99a-5p expression could distinguish PDAC patients with short progression free survival (PFS) after surgery. In situ hybridization of miR-125b-5p and miR-99a-5p in the resected PDAC tissues showed that the miRs are highly expressed in inflammatory cells, mostly consisting of CD79A expressing cells of the B-lymphocyte lineage.

Conclusions: Circulating miR-125b-5p and miR-99a-5p are potential prognostic biomarkers after surgery in patients with PDAC, that reflect an altered immune landscape in response to cancer recurrence.

INTRODUCTION

Pancreatic ductal adenocarcinoma (PDAC) is expected to become the second most frequent cause of cancer death by 2030 [1]. Approximately 15% of patients have resectable disease (stage I or II), whereas more than half of patients have unresectable PDAC [2]. Although PDAC can be removed surgically in early stage disease, the 5-year survival rate of patients that undergo surgical resection is still only 10% [3-5]. After surgery, adjuvant chemotherapy such as gemcitabine treatment is indicated. However, approximately half of the patients are not able to receive adjuvant chemotherapy due to health deterioration [6]. Also, rapid development of metastases shortly after removal of the primary tumor occurs in a subset of PDAC patients. Clinical follow up uses CT imaging, whereas molecular markers of PDAC progression during follow up remain underexplored. Since collection of tissue biopsies from the pancreas is risky, minimally invasive biomarkers attainable as 'liquid biopsies' from blood draws are sorely needed to aid in prognostic stratification of patients and possible adjustment of the treatment regimen. Here we describe circulating, cell free nucleic acids as potential biomarkers.

Mature microRNAs (miRs) are highly conserved short strands of non-coding RNA that regulate gene expression. To date, more than 2600 human mature miRs have been identified and annotated [7], with more than half of human protein-coding genes likely regulated by at least one miR [8]. MiRs are dysregulated in cancer and play crucial roles in immune function, cell proliferation, apoptosis, metastasis, angiogenesis and tumor-stroma interactions [9-11]. It is noteworthy that miRs released from cells can induce miR-mediated gene expression alterations in neighboring as well as in distant cells when entering the circulation [12,13]. In the circulation, miRs are relatively stable and easy to measure, which has inspired a vast amount of biomarker research. The majority of research on circulating miR signatures in oncology is focused on diagnostics [14-18], however miRs can provide crucial insights into cancer progression and the effects of therapeutic interventions [19-22]. In the present study, we profiled serum miRs in patients with PDAC who underwent tumor resection, and in a transgenic mouse model of PDAC progression, to identify novel circulating biomarkers of pancreatic cancer progression.

MATERIAL AND METHODS

Serum miR analysis in KPC mice

The animal experiment with the genetically engineered *LSL-Kras*^{G12D/+}; *LSL-Trp53*^{R172H/+}; *P48-Cre* or KPC mice [23] in this study was approved by the Georgetown University Institutional Animal Care and Use Committee (IACUC). Twelve KPC mice were euthanized at the age of 5 months before ~ 1 mL blood was collected via intracardial puncture in Serum

Z-Gel tubes with clotting activator (Sarstedt). The serum tubes were inverted 5 times and centrifuged at 10,000 x g for 15 minutes. Afterwards the serum was stored in aliquots at -80 °C until further analyses. In addition, pancreas, liver and lungs were collected and processed by formalin fixation and paraffin embedding (FFPE). Tissues were stained with hematoxylin and eosin (H&E) and the slides were examined by a pathologist to evaluate pancreatic neoplasia and to determine the tumor stages. The animals were then divided into two groups based on disease progression: one group with PanIN-3 lesions as the worst disease stage, and a second group with mice that had invasive pancreatic cancer as well as lymph nodes, liver and lung metastases.

Equal volumes of serum samples from the mice belonging to the same group were pooled together, followed by miR isolation using the miRCURY RNA Isolation Kit for Biofluids (Exiqon). The murine miRs were reverse transcribed to cDNA using the miRCURY LNA™ Universal RT microRNA PCR, Polyadenylation and cDNA synthesis kit II (Exiqon). Expression of 179 miRs was analyzed with the qPCR-based Serum/Plasma Focus microRNA PCR Panel (Exiqon) using the ExiLENT SYBR® Green master mix (Exiqon). MiRs with Ct values higher than 30 cycles were excluded, resulting in 154 miRs that were evaluated. The median miR expression value in each pooled serum sample was used to normalize for miR expression. The fold differential expression for each miR was calculated ($2^{-\Delta\Delta Ct}$) and plotted using Prism Graphpad 5.01.

Patient blood collection

All patients provided written informed consent for participation and the protocols associated with this research were approved by the Erasmus Medical Center Medical Ethical Committee (MEC2017-1203). Peripheral venous blood samples were obtained from patients with treatment-naïve resectable PDAC 1 day before pancreaticoduodenectomy and ~4 weeks (range 2-6) after resection. Patients who had prior gastro-intestinal malignancies were excluded. For each serum sample, a total of 8.5 mL of venous blood was collected in SST II Advance serum tubes (BD) with clot activator of silica particles to induce coagulation. After inverting the tubes 6 times, the samples were spun within 4 hours after blood draw at 1258 g for 10 min at 4 °C in a swing-bucket centrifuge (Eppendorf 5810R). The serum was divided in 1 mL aliquots and stored at -80°C until further analyses.

Patients serum miR quantitation

Cell-free circulating miRs from the patients were isolated from 200 µL serum using the miRNeasy serum/plasma miRNA Isolation Kit (Qiagen). Two proprietary pre-mixed spike-in ~20 nt control RNAs (MiRXES) with sequences distinct from annotated mature human miRNAs (miRbase version21) were added into the lysis buffer prior to sample miR isolation, in order to evaluate RNA isolation efficiency. Serum miRs were isolated per manufacturer's

recommendation (Qiagen) and eluted in 15 µL nuclease free water. MiRs were reverse transcribed using IDEAL miR-specific oligos in a multiplex reaction per manufacturer's instruction (MiRXES). In brief, up to 2 µL sample RNA was mixed together with 1 µL RT Spike-in RNA, RT Buffer, nuclease free water, Reverse Transcriptase and a maximum of 10 different miR-specific RT oligos into 20 µL reactions and incubated at 42 °C for 30 min followed by heat inactivation at 95 °C for 5 min, in a SimpliAmp thermal cycler (Applied Biosystems). cDNA was stored at -20 °C (up to 4 weeks) and thawed only once. Before miR quantitation, the cDNA was diluted 1:10 in nuclease free water.

For the quantitative PCRs, 5 µL of sample cDNAs were mixed with the individual miRNA qPCR Assays (MiRXES), nuclease free water and the IDEAL miRNA qPCR Master Mix containing the passive reference dye ROX, into reactions of 20 µL volume. PCR amplifications in the 7500 Fast Real-Time PCR System (Applied Biosystems) were performed using the following protocol: 10 minutes at 95 °C, 5 minutes at 40 °C, followed by 40 cycles of: 10 seconds at 95 °C and 30 seconds at 60 °C with FAM fluorescence reading at the end of this step. The raw threshold cycle (Ct) values were determined using the 7500 Software (Applied Biosystems) with automatic baseline setting. Technical variations introduced during RNA isolation and the process of RT-qPCR were normalized using the measurements of the spike-in control RNAs.

In screen 1 two hundred fifty miRs were measured in n=3 patients before and after surgery. The Ct value cutoff was 33 cycles to ensure reliability of the measurements. MiR levels in screen 1 were normalized using the mean expression value of all measured miRs per sample. From miR screen 1, 44 miRs were selected for further analyses based on the following two criteria: 1.) differential expression before and after surgical tumor removal; 2.) differential regulation after resection in patients with different progression free survival.

Next, the selected 44 miRs plus an additional 12 miRs we identified from the literature were measured in a second cohort of n=10 patients. Two stably expressed reference genes from miR screens 1 and 2 were selected for normalization: miR-29c-5p and miR-421 expression was used because they represent the mean miR expression values in all our patient serum samples. This approach to miR normalization was described by Mestdagh et al. [24]. Potential prognostic miRs were selected according to the two criteria described above. In a third patient cohort (n=15) sixteen miRs were measured, including the two reference genes miR-29c-5p and miR-421.

Data analysis

Patient data were collected during the standard clinical follow up and included patient age, sex, treatment type and timing, resection information, pathological TNM-stage, time to

death, new co-morbidities, time to progression and type of progressive disease. The qPCR Ct values were processed in Excel and converted to fold expression using $2^{-\Delta\Delta C_t}$, normalized to the median miR expression (in the KPC mice and patient screen 1 analyses), or to the expression of reference miR-29c-5p and miR-421 (in the patient screens 2 and 3). The pre- and post-surgery serum miR expression values were presented and analyzed in Prism Graphpad 5.01 and compared between three patient groups: patients with short PFS (0-8 months); median PFS (8-16 months) and long PFS (>16 months). MiRs that were differentially expressed between the patients with short versus long PFS within all three patient cohorts were considered as potential prognostic miRs. The pre- and post-surgery expression values of the selected miRs in patients from all cohorts were analyzed by single factor ANOVA comparing the short (red) versus long (green) PFS patient groups. Kaplan-Meier graphs of PFS for patients with high versus low post-surgery serum miR-122-5p; 125b-5p or 99a-5p expression values compared were analyzed by Chi square (Logrank) test. The cutoff for high and low expression of each miR is based on the median post-surgery expression of the respective miR in all 28 patients.

In situ hybridization (ISH) of FFPE pancreatic cancer tissues

Pancreaticoduodenectomy tissue specimens were collected at the Erasmus Medical Center for clinical pathology evaluation. Stored FFPE tissue blocks were analyzed for clinical histopathological diagnosis. Residual material was used for biomarker analysis. Four μm thick tissue sections on extra adhesive glass slides (Leica, Biosystems) were processed in the Discovery Ultra instrument (Ventana, Roche). The following automated Discovery Universal protocol was used: tissues were preheated at 70 °C for 4 minutes then deparaffinized at 70 °C for 12 min. Pretreatment was performed with CC1 for 16 minutes (Cat. # 950-224, Ventana). One drop of DISC inhibitor (Cat. # 760-4840, Ventana) was applied and incubated for 12 min. The 3' and 5' - DIG labeled miRCURY LNA miRNA Detection probes (Qiagen, hsa-miR-125b-5p cat. # YD00611756-BCG; hsa-miR-99a-5p cat. # YD00619276-BCG; positive control hsa-U6 cat. # YD00699002-BCG and negative control Scramble-miR cat. # YD00699004-BCG) were diluted in formamide-free MiRCURY LNA miRNA ISH Buffer (Qiagen cat. # 339450) to a final 20 nM concentration, applied to the slides and incubated for 8 minutes. Denaturation was established at 90 °C for 8 min, followed by hybridization for 1 hour (at 55 °C for miR-125b-5p; 53 °C for miR-34a-5p; 52 °C for miR-99a-5p; 54 °C for U6 and at 57 °C for the Scramble-miR). Slides were washed twice with SCC (DISCOVERY Ribowash 1x cat. # 760-105, Ventana) and heated to 55 °C for 8 min. Slides were washed and heated again to 55 °C for 8 min. One drop of anti-DIG HRP enzyme conjugate (Cat. # 760-4822, Ventana) was applied and incubated for 16 min. Discovery amplification was performed using one drop of DISC AMP TSA BF and one drop of DISC AMP H2O2 BF (Cat. # 760-226, Ventana) for 32 min of incubation. One drop of DISC anti-BF HRP (cat#760-4828, Ventana) was incubated 16 min, followed by

one drop of DISC Ag C silver (Cat. # 760-227, Ventana) incubation for 16 min. The tissues were counterstained with Hematoxylin II (Cat. # 790-2208, Ventana) for 8 min, followed by incubation with Bluing Reagent Post Counterstain (Cat. # 760-2037, Ventana) incubation for 4 min. Adjacent tissue sections were stained with Hematoxylin and Eosin (H&E). The slides were scanned using the Nanozoomer 2.0-HT slide imager (Hamamatsu).

Immunohistochemistry for CD79A human pancreatic cancer tissues

Immunohistochemistry was performed with an automated immunohistochemistry staining system (Ventana BenchMark ULTRA, Ventana Medical Systems) using the 3,3'-diaminobenzidine method. In brief, following deparaffinization and heat-induced antigen retrieval for 64 min, the tissue sections were incubated with a rabbit monoclonal antibody raised against human CD79A (clone EP82, ready to use, Cell Marque) for 32 minutes at 36 °C. A subsequent amplification step was followed by incubation with hematoxylin II counter stain for 8 min and then a blue-colouring reagent for 8 min according to the manufacturer's instructions (Ventana). The slides were scanned using the Nanozoomer 2.0-HT slide imager (Hamamatsu).

RESULTS

Changes in serum miRs during pancreatic cancer progression in KPC mice

The *LSL-Kras*^{G12D/+}; *LSL-Trp53*^{R172H/+}; *P48-Cre* or KPC transgenic mouse model develops metastatic PDAC that recapitulates the human disease [23]. We investigated the serum miR expression in mice with PanIN lesions and mice with metastatic PDAC to assess whether serum miRs are altered during cancer progression. For this purpose we collected serum from KPC mice at 5 months of age and first evaluated the histology of the pancreas (Fig. 1a), lung and liver tissues (Fig. 1b). Serum from mice (n=3) with PanIN-3 as the highest grade component of lesions in the pancreas and from mice with metastatic PDAC (n=3) was combined into two pooled samples. The two pooled serum samples were analyzed for expression of 179 mature miRs by q-PCR. The 154 miRs that were detected in the serum of mice with metastases were then compared to those in mice with preinvasive PanIN-3 lesions (Supplementary Fig. 1). We found that fourteen serum miRs are downregulated more than 3-fold in mice with metastatic disease compared to age-matched mice with only preinvasive lesions, whereas thirteen miRs are upregulated >3-fold in the serum of mice with PDAC metastases (Table 1). Strikingly, the circulating miR that is upregulated the most in progressive cancer, miR-122-5p, is altered more than 22-fold. These findings indicate that serum miR expression is impacted during cancer progression which we further evaluate in human patients with PDAC.

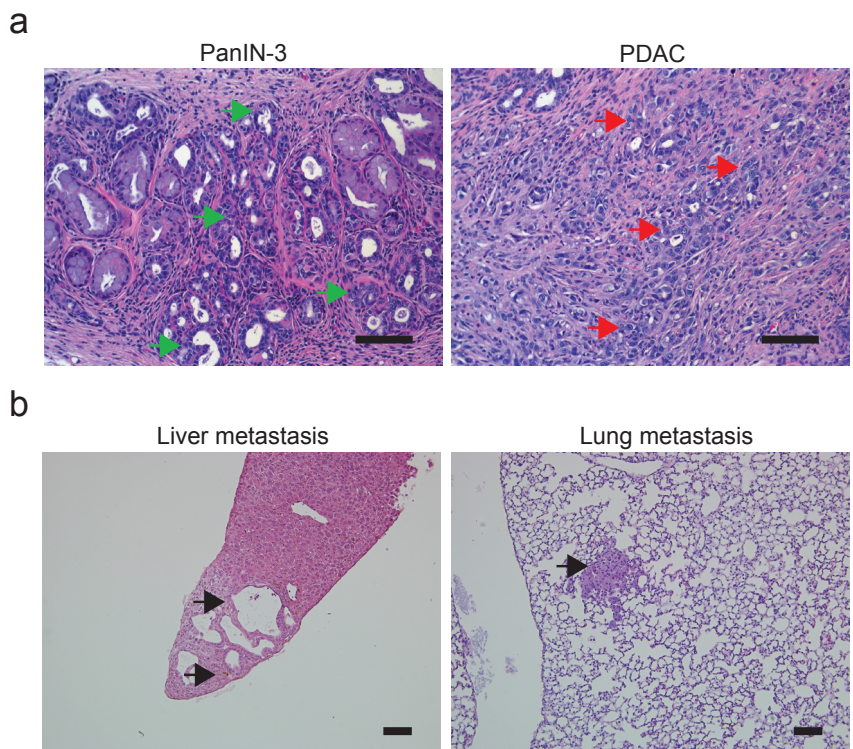


Figure 1. KPC mice with different stages of pancreatic neoplasia at the age of 5 months. (a) Images of formalin fixed, paraffin embedded (FFPE), H&E stained pancreatic tissues obtained from *LSL-Kras^{G12D/+}; LSL-Trp53^{R172H/+}; P48-Cre* (KPC) mice at the age of 5 months. PanIN-3 lesions are indicated by the green arrows, invasive pancreatic cancer is indicated by the red arrows. 20X magnification, scale bar = 100 μ m. (b) Images of FFPE, H&E stained liver and lung tissues from KPC mice at the age of 5 months. Metastatic pancreatic cancer lesions are indicated by the black arrows. 10X magnification, scale bar = 100 μ m.

Table 1. Differentially expressed serum miRs in KPC mice with pancreatic cancer metastases compared to mice with pre-invasive PanIN-3 lesions.

Serum miR	Fold down-regulation	Serum miR	Fold upregulation	Serum miR	Fold down-regulation	Serum miR	Fold upregulation
miR-15a-5p	-7.69	miR-122-5p	22.63	miR-25-3p	-3.45	miR-125a-5p	5.13
miR-451a	-7.69	miR-125b-5p	8.22	miR-93-5p	-3.33	miR-99a-5p	5.03
miR-15b-5p	-6.25	miR-133a	5.94	miR-16-5p	-3.23	Let-7b-3p	4.26
miR-142-3p	-5.88	miR-133b	5.82	miR-19a-3p	-3.23	miR-145-5p	3.86
miR-186-5p	-4.17	miR-10b-5p	5.28	miR-148b-3p	-3.13	miR-28-3p	3.46
miR-103a-3p	-3.85	miR-99b-5p	5.21	miR-20a-5p	-3.03	miR-143-3p	3.41
Let-7i-5p	-3.70	miR-365a-3p	5.17	miR-425-5p	-3.03		

Changes in serum miRs after tumor resection in patients with pancreatic cancer

Next, we analyzed pre- and post-pancreaticoduodenectomy serum from patients with resectable PDAC (n=28) who underwent surgery at the Erasmus Medical Center Rotterdam, in the Netherlands between 2013 and 2017. Patient characteristics are summarized in Table 2. Our aim was to assess the change in serum miR expression after surgery in patients with different progression free survival (PFS). In order to measure miR levels we used a novel technology that allows for exceptionally miR-specific and sensitive quantitative Real Time PCR [25]. The IDEAL assay from MiRXES is explained in Fig. 2a and utilizes miR-specific reverse transcription, as well as a combination of a miR-specific forward and reverse primer to detect and quantitate specific miRs. Details of the approach are shown in Fig. 2b. We initially profiled 250 miRs before and after primary tumor resection in 3 patients with PFS of 7, 11 or 18 months. The miRs that were measured in screen 1 are listed in Supplemental Table 1. From the 250 miRs, 190 were detected by qPCR and only 44 miRs were differentially altered after surgical tumor removal in the patients with different PFS. In a second cohort of PDAC patients (n=10), we measured the 44 informative miRs from screen 1, and an additional 12 miRs that were selected from the literature (Supplemental Table 2). We again compared the change in serum miR expression after surgery to the PFS. From this analysis, we found that 14 miRs can indicate disease progression after surgery. To test this in an independent third cohort of patients (n=15), we measured the levels of these 14 selected miRs (miR-122-5p, miR-125b-5p, miR-34a-5p, miR-99a-5p, miR-146b-5p, miR-154-5p, miR-379-5p, 193b-3p, miR-186-5p, miR-450a-5p, miR-301a-3p, miR-99b-5p, miR-181a-2-3p and miR-130a-3p) before and after surgery. When taking the miR measurements of all 28 pancreatic cancer patients together, we found that only miR-122-5p, miR-125b-5p and miR-99a-5p show a differential expression after surgery in patients with different PFS (Fig. 3a). Although the differential changes in expression of miR-122-5p, miR-125b-5p and miR-99a-5p did not reach statistical significance, these three miRs increase after tumor resection in patients who develop progressive cancer within 8 months, and decrease after tumor resection in patients who have a long PFS of more than 16 months (Fig. 3a). The Kaplan-Meier curves in Fig. 3b show post-surgery serum miR levels in relation to the progression free survival of the 28 patients that were analyzed. Despite the fact that miR-122-5p is upregulated 22-fold in KPC mice with metastatic disease, miR-122-5p is not differentially expressed in patients with short versus long PFS after surgery (Fig. 3b). On the other hand, patients with high serum levels of miR-125b-5p or miR-99a-5p after surgery have a significantly worse prognosis (Fig. 3b). In summary, we found that miR-125b-5p and miR-99a-5p are prognostic circulating biomarkers in KPC mice and in patients with pancreatic cancer.

Table 2. Patient characteristics.

Patient ID	cohort	Disease stage	Serum time point [days]	PFS [months]	Progressive disease sites	OS [months]	Received therapy	Age [years]	Gender
001NT003	1	resectable PDAC pT3N0 R0	pre surg						
001NT005			post surg [11]	18.0	local; peritoneal	32.2	Whipple / adjuv gemcit / pall gemcit nab-paclitaxel	74	m
001PP011	1	resectable PDAC pT3N1 R0	pre surg						
001PP012			post surg [15]	6.5	local; lymph nodes	8.2	Whipple / adjuv gemcit	76	m
001NT017	1	resectable PDAC pT3N1 R1	pre surg						
001NT018			post surg [15]	10.9	local; osseous	14.5	Whipple / adjuv gemcit	73	f
001PP007	2	resectable PDAC pT3N0 R0	pre surg						
001PP008			post surg [15]	6.6	local; peritoneal	15.9	Whipple / adjuv gemcit	55	f
001PP009	2	resectable PDAC pT3N1 R0	pre surg						
001PP010			post surg [14]	7.1	peritoneal; lung	12.9	Whipple / adjuv gemcit	73	m
001PP036	2	resectable PDAC pT3N1 R0	pre surg						
001PP043			post surg [36]	5.0	liver	5.7	Whipple	71	f
001NT113	2	resectable PDAC pT3N1 R0	pre surg						
001NT118			post surg [27]	> 25.6		> 25.6	Whipple / adjuv gemcit	71	m
001PP048	2	resectable PDAC pT3N1 R0	pre surg						
001PP053			post surg [28]	29.6	local; lymph nodes; lung	>29.6	Whipple / adjuv gemcit	58	m
001NT115	2	resectable PDAC pT3N1 R1	pre surg						
001PP034			post surg [22]	5.23	local; liver	10.4	Whipple / adjuv gemcit	71	m
001PP041	2	resectable PDAC pT3N1 R1	pre surg						
001PP050			post surg [35]	> 30		> 30	Whipple / adjuv gemcit	74	m
001PP032	2	resectable PDAC pT3N0 R0	pre surg						
001PP039			post surg [30]	11.8	omental; liver; lung	31.5	Whipple / adjuv gemcit / pall FOLFIRINOX / IL1RAP inhibitor	60	m
001NT133	2	resectable PDAC pT3N1 R1	pre surg						
001NT137			post surg [25]	13.9	local; peritoneal; liver	16.6	Whipple / adjuv gemcit / pall FOLFIRINOX	59	m
001PP028	2	resectable PDAC pT3N1 R0	pre surg						
001PP030			post surg [22]	8.6	local; liver	15.1	Whipple / adjuv gemcit	78	f



Table 2. Patient characteristics. (continued)

Patient ID	cohort	Disease stage	Serum time point [days]	PFS [months]	Progressive disease sites	OS [months]	Received therapy	Age [years]	Gender
001PP072	3	resectable PDAC pT3N0 R1	pre surg	12.1	liver	> 17	Whipple / adjuv gemcit	63	m
001PP073			post surg [20]						
001PP077	3	resectable PDAC pT3N1 R0	pre surg	> 16		> 16	Whipple / adjuv gemcit	51	m
001PP082			post surg [27]						
001INT177	3	resectable PDAC pT3N0 R1	pre surg	13.2	local; peritoneal; omental	15.1	Whipple / adjuv gemcit	69	m
001INT183			post surg [22]						
001INT143	3	resectable PDAC pT3N1 R1	pre surg	8.4	liver	16.9	Whipple / adjuv gemcit	72	m
001INT148			post surg [27]						
001INT236	3	resectable PDAC pT3N1 R1	pre surg	0.9	local; peritoneum; lungs; liver	2.1	Whipple / adjuv gemcit	72	f
001INT245			post surg [26]						
001INT235	3	resectable PDAC pT3N1 R1	pre surg	> 16		> 16	Whipple	84	m
001INT246			post surg [29]						
001INT158	3	resectable PDAC pT3N1 R1	pre surg	> 24		> 24	Whipple	87	f
001INT161			post surg [48]						
001INT167	3	resectable PDAC pT3N1 R0	pre surg	16.1	lungs; liver	> 23	Whipple / adjuv gemcit	73	m
001INT173			post surg [27]						
001INT217	3	resectable PDAC pT3N1 R0	pre surg	1.9	local; lymph node; liver	2.4	Whipple	68	m
001INT223			post surg [26]						
001INT178	3	resectable PDAC pT3N1 R0	pre surg	18.9	local; lymph node	> 18.9	Whipple / adjuv gemcit-capecit	70	m
001INT187			post surg [22]						
001INT171	3	resectable PDAC pT3N1 R1	pre surg	9.7	local; mesenteric; lungs; liver	> 9.7	Whipple / gemcit	73	m
001INT175			post surg [31]						
001INT128	3	resectable PDAC pT3N1 R1	pre surg	9.5	local; liver	16.2	Whipple / adjuv gemcit	55	m
001INT134			post surg [34]						
001INT110	3	resectable PDAC pT3N1 Rx	pre surg	16.0	local; liver	18.5	PPPD / adjuv gemcit	71	m
001INT121			post surg [36]						

Table 2. Patient characteristics. (continued)

Patient ID	cohort	Disease stage	Serum time point [days]	PFS [months]	Progressive disease sites	OS [months]	Received therapy	Age [years]	Gender
00INT212	3	resectable PDAC pT3N1 R1	pre surg	0.1	local; liver	4.3	PPPD / RT	84	m
00INT221			post surg [36]						
00INT152	3	resectable PDAC pT3N1 R1	pre surg	7.7	peritoneal; lymph node	8.2	Whipple	66	m
00INT156			post surg [34]						

ID = identification; PDAC = pancreatic ductal adenocarcinoma; p = pathological; T = Tumor stage; No = lymph node metastases; N1= lymph node metastases; Ro = cancer free resection margins; R1 = cancer in resection margins; surg = surgery; PFS = progression free survival after surgery; OS = overall survival after surgery; RT = radiotherapy; Whipple = pancreaticoduodenectomy; PPPD = pylorus-preserving pancreaticoduodenectomy; adjuv = adjuvant; gemcit = gemcitabine; nab-paclitaxel = nanoparticle albumin-bound paclitaxel; IL1RAP = Interleukin 1 Receptor Accessory Protein; capecit = capecitabine; Age at time of surgery; m = male; f = female.



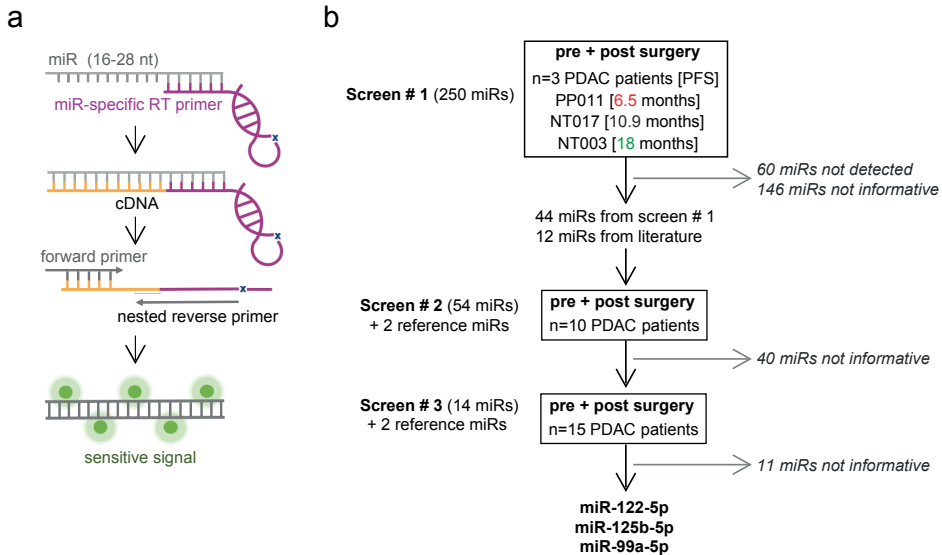


Figure 2. Analysis approach of prognostic miRs in the serum of patients with resectable pancreatic cancer. (a) Schematic of the IDEAL real time RT-PCR assay from MiRXES. MiR-specific reverse transcription (RT) and a miR-specific pair of forward and reverse primers lead to high specificity and sensitive PCR signals. miR = microRNA; nt = nucleotides; RT= reverse transcription; cDNA = complementary DNA. (b) Overview of performed serum miR analysis in patients with resectable pancreatic ductal adenocarcinoma (PDAC) to identify indicators of progression free survival (PFS) after surgical tumor removal.

MiR-125b-5p and miR-99a-5p are highly expressed in inflammatory cells in human resected pancreatic cancers

In order to assess the expression of miR-125b-5p and miR-99a-5p further, we analyzed the resected pancreatic cancer tissues by in situ hybridization (ISH) with DIG-labeled locked nucleic acid miR probes. The positive and negative controls for the ISH assays are shown in Supplemental Figure 2. MiR-125b-5p is expressed at low levels in the cytoplasm of normal acinar cells, as well as in a fraction of the PanIN cells (Fig. 4a). However, a small fraction of cells in the stroma surrounding the invasive cancer cells express high levels of miR-125b-5p (Fig. 4b). There is no difference in the number of miR-125b-5p-high stroma cells in tumors from patients with short versus long PFS. Interestingly, the miR-125b-5p-high cells pertain in inflammatory cell aggregates in the tumor stroma and are located within clusters of CD79A positive cells (Fig. 4b), indicating that miR-125b-5p may play a role in B-lymphocyte/ plasma cell infiltration in pancreatic cancer stroma. MiR-99a-5p expressing cells are less abundant than miR-125b-5p positive cells in the pancreatic tumors. MiR-99a-5p positive cells are only present in limited regions of tumor stroma, specifically in muscular and connective tissue where pancreatic cancer cells invade into. Fig. 5 shows tumor regions with cells that express high levels of miR-99a-5p. In the centers of the pancreatic cancers

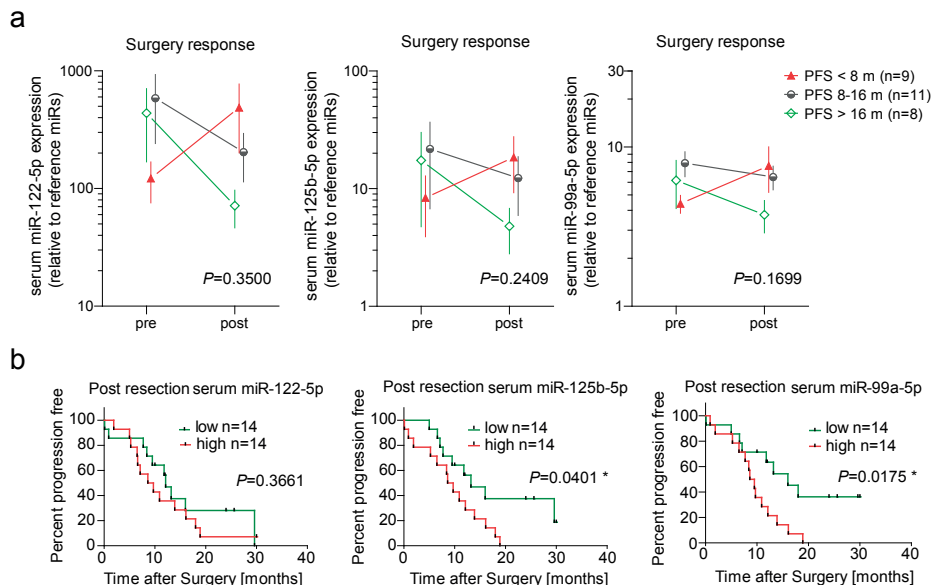


Figure 3. Expression levels of three serum miRNAs in pancreatic cancer patients with different outcomes. (a) Average expression levels of serum miRNAs 122-5p, 125b-5p or 99a-5p before and after surgery in 3 groups of patients with different progression free survival (PFS) duration. Serum miR values were normalized to the average expression of reference miR-29c-5p and miR-421 for each sample. Note the log scale of the Y-axis. Error bars are SEM, P -values by single factor ANOVA comparing the short (red) versus long (green) PFS patient groups. (b) Kaplan-Meier graphs of PFS for patients with increased or decreased serum miR-122-5p, 125b-5p or 99a-5p levels after surgical tumor removal. P values by Chi square (Logrank) test.

there are no cells that express miR-99a-5p. When comparing the location of CD79A positive cells in the adjacent tissue slides, we observed that the miR-99a-5p expressing inflammatory cells are in close proximity to cells of the B-cell lineage (Fig. 5).

In summary, we found that high expression of serum miR-125b-5p and miR-99a-5p is associated with pancreatic cancer progression in transgenic mice as well as in patients after surgical tumor removal. MiR-125b-5p as well as miR-99a-5p is highly expressed in a subset of inflammatory cells in the pancreatic tumor stroma, and are associated with cells from the B-lymphocyte lineage. The abundance of inflammatory cells expressing high levels of miR-125b-5p or miR-99a-5p in the tumor tissues was not different in patients with short versus long progression free survival.

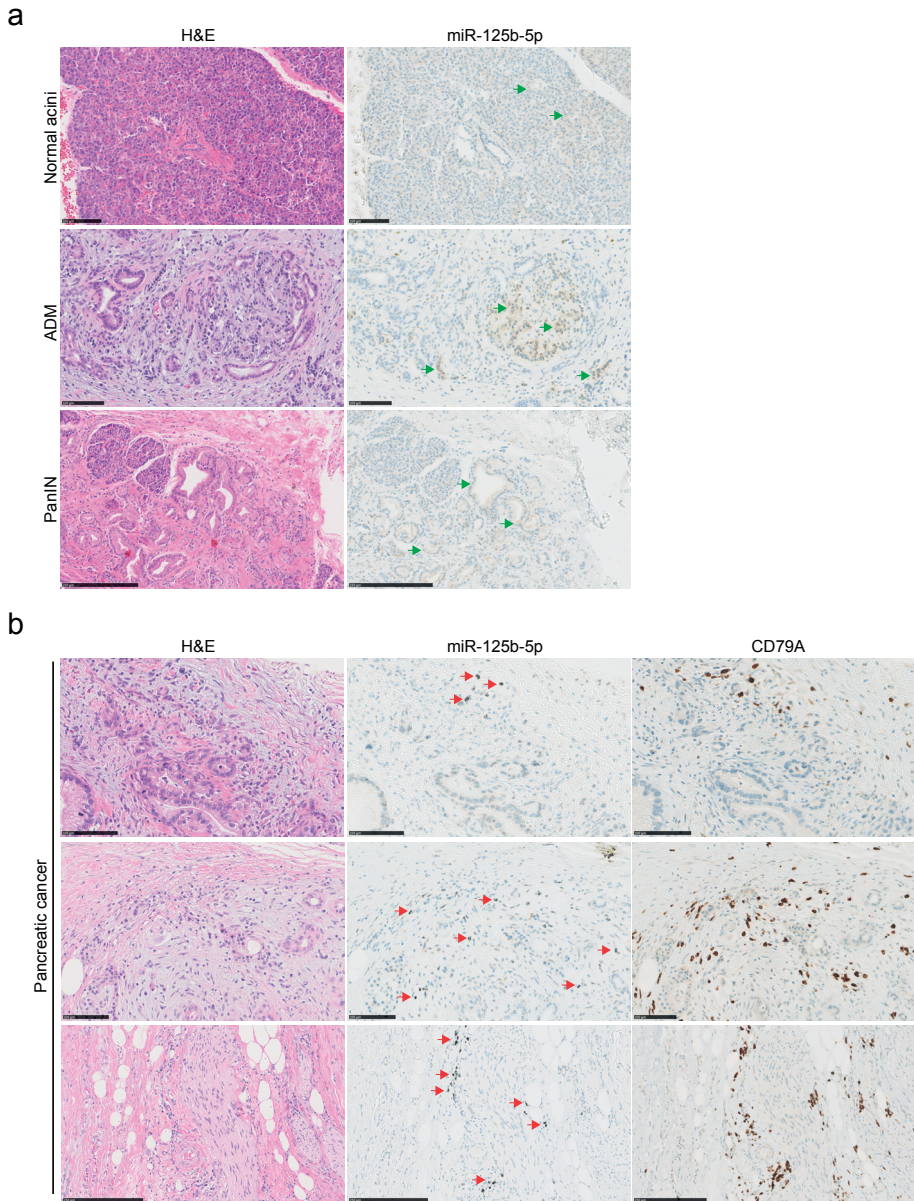


Figure 4. MiR-125b-5p detection by in situ hybridization in pancreatic cancer tissues. Images of resected pancreas tissues from patients with pancreatic cancer. Consecutive FFPE tissue sections were stained with H&E or a DIG labeled miR-125b-5p probe. MiR-125b-5p expression is detected with silver resulting in brown/black staining, whereas nuclei are stained with Hematoxylin in blue. (a) Representative images of low expression of miR-125b-5p, (green arrows), in untransformed pancreatic acinar cells and cells that underwent acinar to ductal metaplasia (ADM) or pancreatic intraepithelial neoplasia (PanIN). (b) Representative images of cells in the tumor stroma with high expression of miR-125b-5p (red arrows). Corresponding tissue sections are stained with H&E and B-lymphocyte marker CD79A.

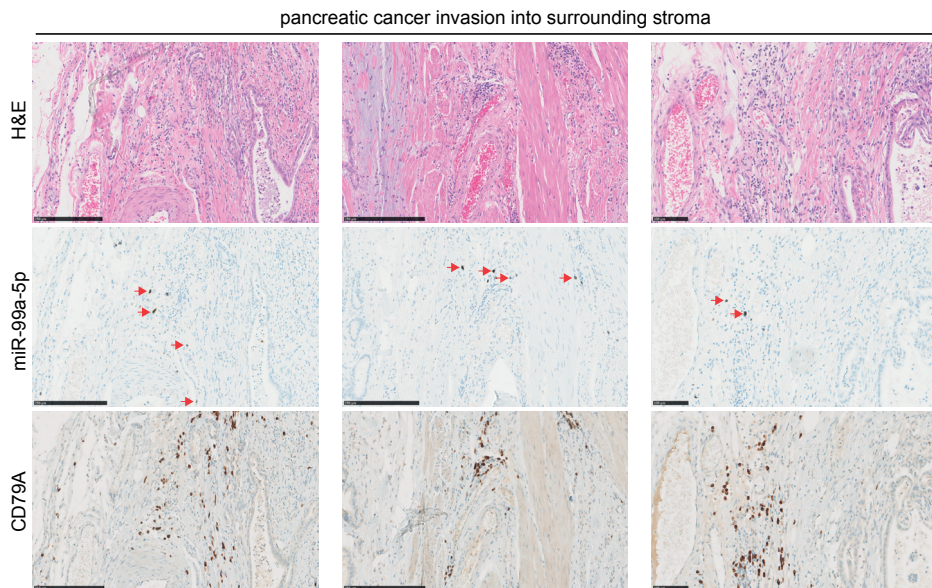


Figure 5. MiR-99a-5p detection by in situ hybridization in pancreatic cancer tissues. Images of resected pancreas tissues from patients with pancreatic cancer. Consecutive FFPE tissue sections were stained with H&E or a DIG labeled miR-99a-5p probe, or a B-lymphocyte marker CD79A. Red arrows indicate miR-99a-5p expression, detected with silver resulting in brown/black staining, whereas cell nuclei are stained with Hematoxylin in blue.

DISCUSSION

Until now, approved non-invasive circulating biomarkers for the prognostication of patients with pancreatic cancer are lacking. Clinical follow up of pancreatic cancer patients in the Netherlands is not standardized [26] and currently consists of physical examination and at times radiographical imaging by CT scans which have a low performance in detecting early metastatic disease. Repeated blood draws followed by miR expression analysis that could stratify patients at higher risk for progressive disease and could prompt treatment adjustment would vastly improve patient care. MiRs are suitable candidates for the prediction of cancer progression due to their altered expression during tumorigenesis and their stability in the circulation[22].

Numerous studies have shown that circulating miRs are altered in early PDAC as well as in metastatic PDAC [27]. Zhou *et al.* showed that patients with early PDAC could be distinguished from healthy controls by the plasma upregulation of miR-122-5p; miR-125b-5p; miR-192-5p; miR 193b-3p; miR-122-3p and miR-27b-3p before treatment [14]. In contrast, they found that pre-treatment decreased miR-125b-5p was associated with worse OS. It was recently shown that increased serum expression of the miR-99 family is associated to

pancreatic cancer diagnosis [28]. Studies similar to these, which assess circulating miR levels for the diagnosis of PDAC are difficult to corroborate. Inconsistent results are due to interpatient diversity as well as technical differences in quantitation and data normalization [29].

Unfortunately, a subset of patients with PDAC that undergo primary tumor resection rapidly succumb to disease recurrence, whereas other patients have long progression free survival after surgery. Identifying the patients at risk for early disease recurrence could prompt adjustments in adjuvant treatment decisions and improve patient outcome. In the current study, we performed a prognostic miR biomarker analysis using serum samples of treatment-naïve, resectable PDAC patients. We profiled serum miR expression before and after surgery and compared the changes to the progression free survival of the patients. This comparison highlights the change in serum miR levels after removal of the primary cancer. The prognostic miRs identified in the patients were also indicative of PDAC metastases in the KPC mice, supporting their biologic importance for pancreatic cancer progression.

Genetically engineered mouse models of pancreatic cancer have led to major improvements in the understanding of PDAC development. Specifically, the *LSL-Kras^{G12D/+}; LSL-Trp53^{R172H/+}; P48-Cre* or KPC mice display progressive PDAC that mimics the features of the human disease [23]. KPC mice initially develop preinvasive acinar to ductal metaplasia (ADM) and pancreatic intraepithelial neoplasia (PanIN) lesions before widespread PDAC, all in the presence of an intact immune system. The median survival of KPC mice is 5 months and all mice succumb to the disease before the age of one year [23]. We performed a cross-species comparison of serum microRNA expression: the prognostic miRs we identified in the patients were also correlated to PDAC metastases in the KPC mice, confirming their importance in pancreatic cancer progression.

Circulating miRs that are associated with cancer presence often do not originate from cancer cells themselves. For example, miR-125b expression in colorectal liver and lung metastases is ~3 fold and ~7-fold higher in the stroma than in the cancer cells [30]. Indeed, the majority of circulating miRs are derived from blood cells and the endothelium [31,32]. PDAC progression goes hand in hand with alterations in systemic immune cell profiles [33] and this link between altered circulating miRs during cancer progression and immune cells was confirmed in our study. We found that miR-125b-5p and miR-99a-5p levels are soaring in cells that are closely associated to B-lymphocytes in the tumor stroma. Others have shown that miR-125b-5p is upregulated in B-lymphocytes [34] and can cause leukemia in mice [35,36]. In pancreatic tumors, high levels of infiltrating plasma cells are significantly correlated with worse prognosis in patients after surgery [37]. We found that after surgical tumor removal, patients with high levels of serum miR-125b-5p or miR-99a-5p

have shorter progression free survival. MiR-125b-5p and miR-99a-5p belong to the 20 most abundant miRs in human plasma exosomes [38], indicating that these miRs are actively packaged and released into the bloodstream. Circulating miRs are transferred from cell to cell and can elicit immune modulation [39]. MicroRNA-containing T-regulatory-cell-derived exosomes suppress pathogenic T helper 1 cells [40]. Serum miRs interact more with immune-related mRNA genes than with non-immune related genes [41]. A recent study showed that miR-125b-5p and miR-99a-5p both downregulate the activation of $\gamma\delta$ T-lymphocytes and their cytotoxicity to lymphoma cells [42]. In humans and rats, treatment with methylprednisolone leads to increased plasma miR-99a-5p levels, suggesting miR-99a-5p is involved in systemic immune suppression [43]. Others have shown that miR-99a-5p inhibits the mammalian target of rapamycin (mTOR) signaling in bladder cancer cells [44], which was also described in gastric cancer tissues by Zhang et al. [45]. mTOR is not only an important cancer-related pathway, mTOR is also crucial for hematopoietic cell fate [46,47]. The differentiation of naïve T-cells into distinct effector T cells is promoted by mTOR [46]. In the absence of mTORC1 activity myeloid differentiation is impaired due to a block in glucose uptake and lipid metabolism [48]. Cell-free miR-99a-5p levels are high in the blood of patient with progressive pancreatic cancer, suggesting that the miR is produced at high levels by a subset of leukocytes, and can potentially be taken up by other cells, leading to the abrogation of mTOR among other pathways.

On the other hand, expression of miR-122-5p is liver specific and absent in most other tissues [49-51]. In the KPC mice with metastatic PDAC, miR-122-5p was upregulated 22-fold in comparison to mice with pre-invasive lesions. In the patients who underwent surgical tumor resection serum miR-122-5p levels went up after surgery in patients with early disease recurrence, however post-surgery serum miR-122-5p levels could not distinguish patients based on PFS, or based on the presence of liver metastases. This may suggest that liver damage is present at some level in all patients who undergo pancreaticoduodenectomy for pancreatic cancer.

There has been very little to no research that compares the levels of miRs after surgical removal of primary pancreatic cancers. In our study we compared serum miRs pre and post resection in treatment naïve patients that were operated at the Erasmus Medical Center between 2013 and 2017. Recently it became clear that patients with (borderline) resectable PDAC that undergo preoperative chemo/radiotherapy have a better survival [52,53]. From now on all patients with (borderline) resectable PDAC in the Netherlands will be offered to receive preoperative chemotherapy, if the performance status of the patient permits and the patient is willing to undergo systemic treatment. Chemotherapy has a vast impact on the immune landscape [54,55]. Whether serum miR-125b-5p and miR-99a-5p remains to be predictive of disease progression after surgery in pre-treated patients remains to be

evaluated. Therefore we are currently collecting blood samples to evaluate the changes in the serum miRs of patients with (borderline) resectable patients who undergo pre-operative FOLFIRINOX chemotherapy or gemcitabine/radiotherapy.

In summary, serum miR-125b-5p and miR-99a-5p levels are potential indicators of early disease recurrence after surgery in patients with pancreatic cancer and are likely originating from immune cells. Further dissection of the dynamics and functions of miR-125b-5p and miR-99a-5p in the immune response to pancreatic cancer will provide fundamental information to assist in the development of biomarkers and better immune therapies.

ACKNOWLEDGEMENTS

The authors would like to thank the patients at the Erasmus Medical Center for providing serum for biomarker analyses. The authors also thank Jeroen Versteeg and Narayan Shivapurkar for the useful discussions and part of the groundwork of this study, Bhaskar Kallakury for the histopathological analyses of the murine pancreatic cancers, Judith Verhaagen for the assistance in writing the clinical protocol and collection of clinical data, as well as Buddy Roovers and colleagues for the processing and storage of patient serum samples. We thank MiRXES for measurements of some of the samples analyzed here. This research was funded in part by funds from the Lombardi Comprehensive Cancer Center as well as NIH grants P30 CA51008 (AW), The Ruesch Center for the Cure of GI Cancers (AW and EEV), The Living with Hope Foundation (EEV), The International Fulbright Science and Technology award (IP) and Croatian Graduate Student Foundation Award (IP).

AUTHORS' CONTRIBUTIONS

AW, EEV, IP and CHJE conceived the project. IP and EEV performed the animal studies, MS led the patient care, blood collection and clinical data analyses, TPPB performed the in situ hybridization and immunohistochemistry. The histology was evaluated by pathologist JMK. IP analyzed the murine miR data, EEV analyzed the human miR data and EEV wrote the manuscript. IP, CHJE and MS contributed to edits of the manuscript. All authors reviewed and approved the manuscript.

DISCLOSURES

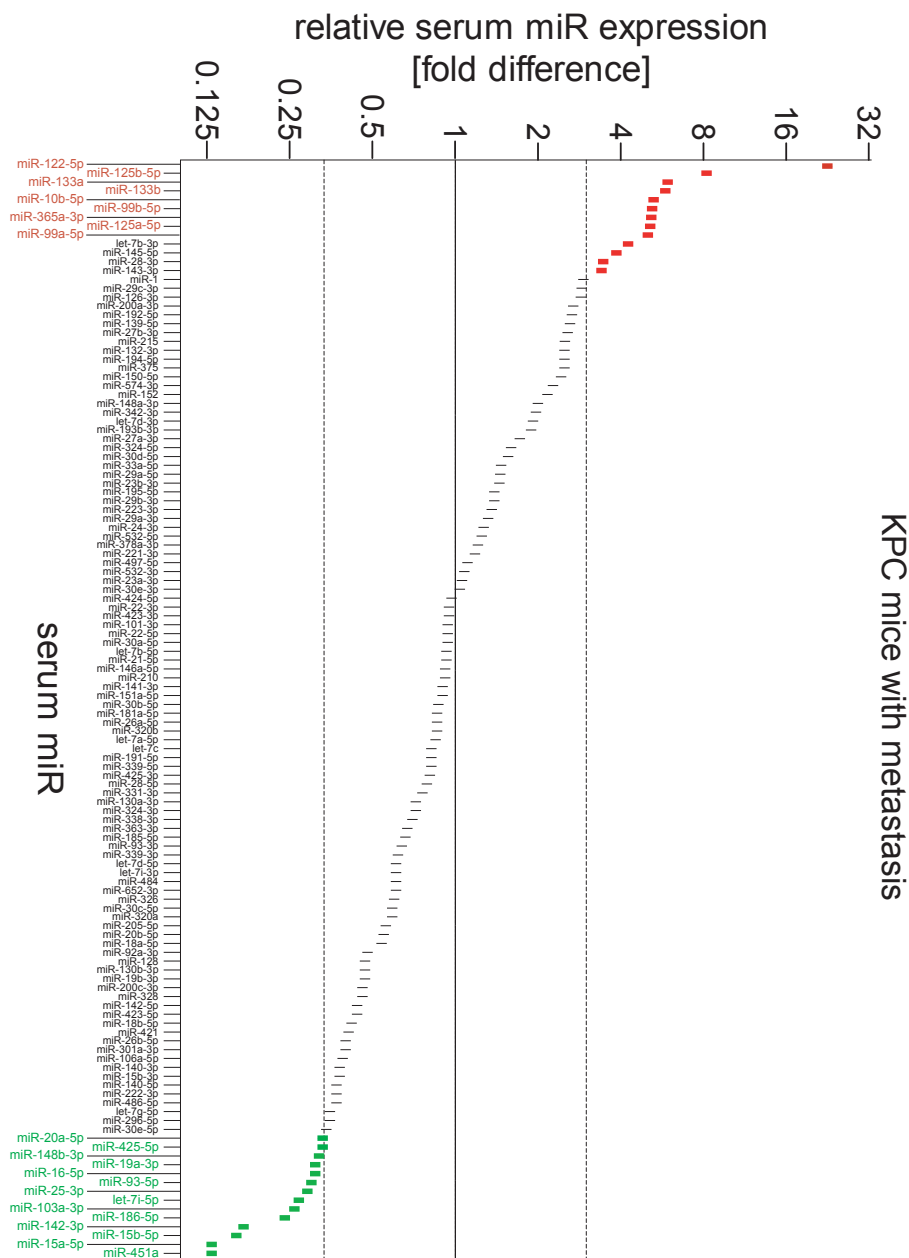
None of the authors have conflicts of interest to disclose.

Supplementary Table 1. List of miRs that were detected in screen # 1 in the serum of n=3 patients with resectable PDAC before and after surgical tumor resection.

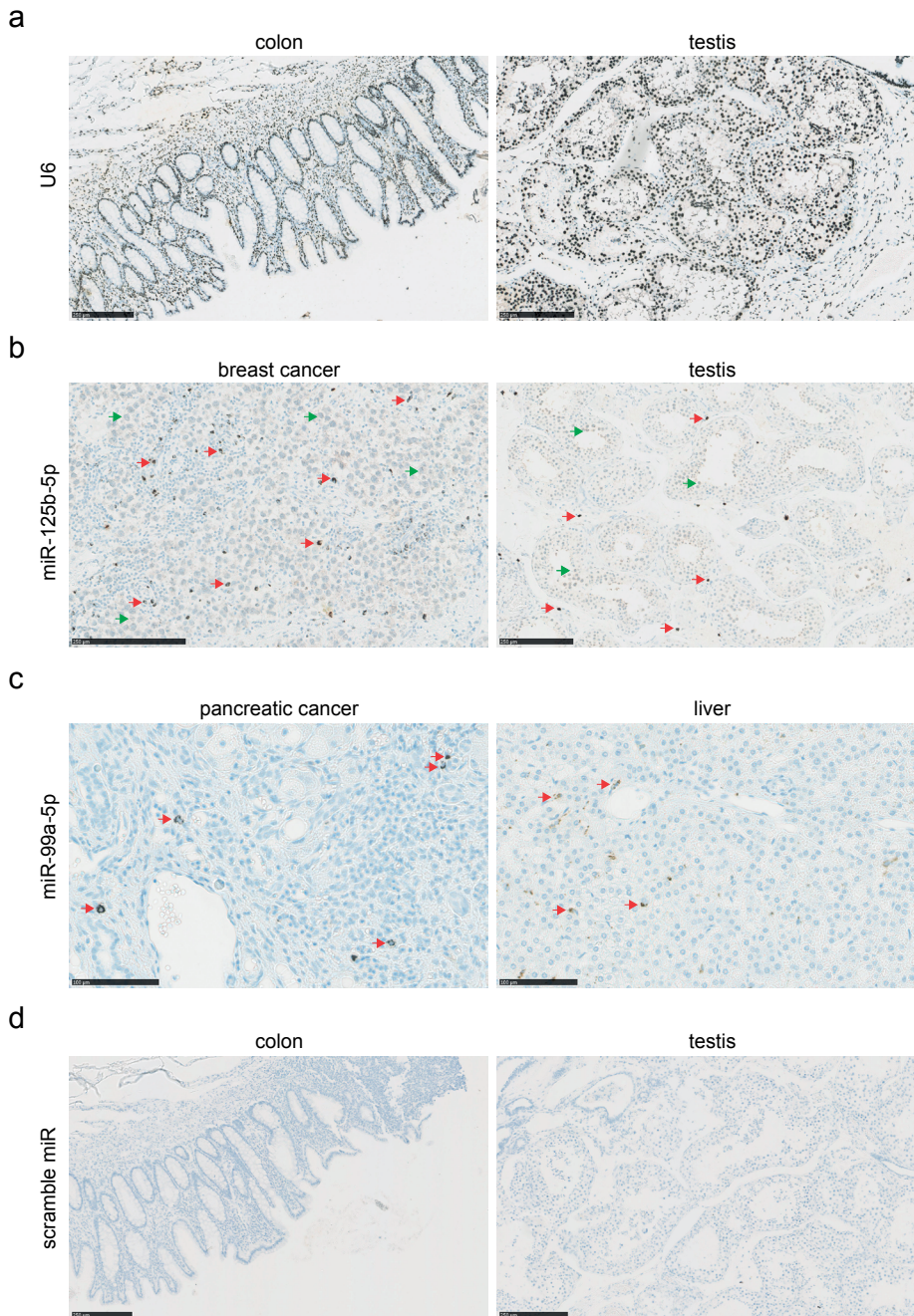
let-7c-5p	let-7d-5p	miR-16-5p	miR-24-3p	miR-99a-5p	miR-150-5p
miR-196a-5p	miR-199a-5p	miR-199a-3p	miR-208a-3p	miR-215-5p	miR-223-3p
miR-200b-3p	miR-15b-5p	miR-27b-3p	miR-30b-5p	miR-125b-5p	miR-128-3p
miR-135a-5p	miR-152-3p	miR-153-3p	miR-191-5p	miR-23b-3p	miR-126-5p
miR-126-3p	miR-154-5p	miR-193a-3p	miR-194-5p	miR-302d-3p	miR-382-5p
miR-328-3p	miR-323a-3p	miR-326	miR-345-5p	miR-409-3p	miR-146b-5p
miR-495-3p	miR-497-5p	miR-518b	miR-92b-3p	miR-181a-2-3p	miR-144-5p
miR-29c-5p	miR-193b-5p	miR-532-3p	miR-885-5p	miR-301b-3p	miR-1246
miR-320d	miR-15a-5p	miR-19b-3p	miR-20a-5p	miR-26a-5p	miR-27a-3p
miR-28-5p	miR-98-5p	miR-29b-3p	miR-106a-5p	miR-192-5p	miR-129-5p
miR-30d-5p	miR-139-5p	miR-10a-5p	miR-181a-5p	miR-224-5p	miR-130a-3p
miR-142-3p	miR-9-3p	miR-125a-5p	miR-17-5p	miR-190a-5p	miR-195-5p
miR-200c-3p	miR-301a-3p	miR-99b-5p	miR-361-5p	miR-378a-5p	miR-330-3p
miR-337-3p	miR-324-3p	miR-338-3p	miR-425-3p	miR-429	miR-452-5p
miR-485-5p	miR-491-5p	miR-21-5p	miR-421	miR-181c-3p	miR-221-5p
miR-223-5p	miR-125a-3p	miR-219a-2-3p	miR-500a-5p	miR-374b-5p	miR-1271-5p
let-7f-5p	miR-19a-3p	miR-25-3p	miR-92a-3p	miR-95-3p	miR-96-5p
miR-10b-5p	miR-34a-5p	miR-103a-3p	miR-199b-5p	miR-122-5p	miR-132-3p
miR-133a-3p	miR-143-3p	miR-145-5p	miR-127-3p	miR-146a-5p	miR-185-5p
miR-186-5p	miR-188-5p	miR-29c-3p	miR-200a-3p	miR-130b-3p	miR-30e-5p
miR-30e-3p	miR-339-5p	miR-335-5p	miR-133b	miR-196b-5p	miR-20b-5p
miR-451a	miR-484	miR-486-5p	miR-193b-3p	miR-493-3p	miR-590-5p
miR-769-5p	miR-140-3p	miR-193a-5p	miR-34b-3p	miR-337-5p	miR-151a-5p
miR-423-5p	miR-616-3p	miR-628-5p	miR-874-3p	miR-1290	miR-1304-5p
let-7a-5p	let-7b-5p	miR-221-3p	miR-22-3p	miR-29a-3p	miR-30a-3p
miR-32-5p	miR-93-5p	miR-100-5p	miR-30c-5p	miR-183-5p	miR-204-5p
miR-205-5p	miR-219a-5p	miR-222-3p	miR-141-3p	miR-134-5p	miR-206
miR-320a	miR-106b-5p	miR-363-3p	miR-365a-3p	miR-370-3p	miR-375
miR-378a-3p	miR-379-5p	miR-151a-3p	miR-148b-3p	miR-324-5p	miR-450a-5p
miR-432-5p	miR-519c-3p	miR-503-5p	miR-539-5p	miR-487b-3p	miR-584-5p
miR-425-5p	miR-21-3p	miR-7-1-3p	miR-34a-3p	miR-106b-3p	miR-99b-3p
miR-362-3p	miR-342-5p	miR-589-5p	miR-1226-3p		

Supplementary Table 2. List of miRs that were measured in screen # 2 in the serum of n=10 patients with resectable PDAC before and after surgical tumor resection.

let-7d-5p	miR-144-5p	miR-28-5p	miR-375	miR-616-5p
let-7g-5p	miR-146b-5p	miR-29c-5p	miR-379-5p	miR-627-5p
let-7i-5p	miR-154-5p	miR-301a-3p	miR-421	miR-651-5p
miR-103a-3p	miR-154-5p	miR-302f	miR-450a-5p	miR-885-5p
miR-122-5p	miR-155-5p	miR-30e-3p	miR-454-3p	miR-9-3p
miR-1226-3p	miR-16-5p	miR-330-3p	miR-486-5p	miR-98-5p
miR-125b-5p	miR-181a-2-3p	miR-34a-3p	miR-491-5p	miR-99a-5p
miR-127-3p	miR-186-5p	miR-34a-5p	miR-493-3p	miR-99b-5p
miR-1285-3p	miR-18a-3p	miR-34b-3p	miR-495-3p	
miR-130a-3p	miR-191-5p	miR-363-3p	miR-584-5	
miR-135b-5p	miR-221-3p	miR-370-3p	miR-590-5p	
miR-140-3p	miR-22-3p	miR-374b-5p	miR-616-3p	



Supplementary Figure 1. Relative expression levels of serum miRNAs in KPC mice with pancreatic cancer metastasis. Serum miRNAs from two groups of *LSL-Kras*^{G12D/+}; *LSL-Trp53*^{R72H/+}; *P48-Cre* (KPC) mice with different disease stage at the age of 5 months were analyzed. Serum from KPC animals with pancreatic cancer metastases (n=3 mice) was pooled and compared to pooled serum from n=3 mice with preinvasive PanIN-3 lesions. 155 microRNAs were detected by qPCR and expression levels were normalized to the median expression value per sample. MiRs that were differentially expressed > 3-fold are highlighted in red and green. Note the log scale for the Y-axis.



Supplementary Figure 2. MiR in situ hybridization (ISH) controls. Images of FFPE tissues that are stained with silver after in situ hybridization of dual-DIG labeled miR probes leading to brown/black staining. Nuclei are stained with Hematoxylin in blue. Scale bars = 250 μ m. (a) U6 expression in human colon and testis tissue, serving as positive controls for the ISH assay. (b) MiR-125b-5p expression in

Her2Neu positive human breast cancer and human testis tissues. Note the distinct staining patterns in the breast cancer cells and Sertoli cells that have low miR-125b-5p expression (green arrows) versus the single cells in the stroma that have high expression (red arrows). (c) MiR-99a-5p expression in human pancreatic cancer and liver. Cells in the stroma with high levels of miR-99a-5p are indicated with the red arrows. (d) Scramble miR expression in human colon and testis tissues, which serves as a negative control for the ISH assay.

REFERENCES

1. Rahib, L., Smith, B. D., Aizenberg, R. et al. (2014) Projecting cancer incidence and deaths to 2030: the unexpected burden of thyroid, liver, and pancreas cancers in the United States. *Cancer Res* 74, 2913-2921
2. Stathis, A. & Moore, M. J. (2010) Advanced pancreatic carcinoma: current treatment and future challenges. *Nat Rev Clin Oncol* 7, 163-172
3. Luberic, K., Downs, D., Sadowitz, B. et al. (2017) Has survival improved following resection for pancreatic adenocarcinoma? *Am J Surg* 214, 341-346
4. van Rijssen, L. B., Koerkamp, B. G., Zwart, M. J. et al. (2017) Nationwide prospective audit of pancreatic surgery: design, accuracy, and outcomes of the Dutch Pancreatic Cancer Audit. *HPB* (Oxford) 19, 919-926
5. Conlon, K. C., Klimstra, D. S. & Brennan, M. F. (1996) Long-term survival after curative resection for pancreatic ductal adenocarcinoma. Clinicopathologic analysis of 5-year survivors. *Ann Surg* 223, 273-279
6. Mayo, S. C., Gilson, M. M., Herman, J. M. et al. (2012) Management of patients with pancreatic adenocarcinoma: national trends in patient selection, operative management, and use of adjuvant therapy. *J Am Coll Surg* 214, 33-45
7. Griffiths-Jones, S., Grocock, R. J., van Dongen, S. et al. (2006) miRBase: microRNA sequences, targets and gene nomenclature. *Nucleic Acids Res* 34, D140-144
8. Krol, J., Loedige, I. & Filipowicz, W. (2010) The widespread regulation of microRNA biogenesis, function and decay. *Nat Rev Genet* 11, 597-610
9. Chen, C. Z., Schaffert, S., Frago, R. et al. (2013) Regulation of immune responses and tolerance: the microRNA perspective. *Immunol Rev* 253, 112-128
10. Lu, L. F. & Liston, A. (2009) MicroRNA in the immune system, microRNA as an immune system. *Immunology* 127, 291-298
11. Lin, S. & Gregory, R. I. (2015) MicroRNA biogenesis pathways in cancer. *Nat Rev Cancer* 15, 321-333
12. Valadi, H., Ekstrom, K., Bossios, A. et al. (2007) Exosome-mediated transfer of mRNAs and microRNAs is a novel mechanism of genetic exchange between cells. *Nat Cell Biol* 9, 654-659
13. Kosaka, N., Iguchi, H., Yoshioka, Y. et al. (2010) Secretory mechanisms and intercellular transfer of microRNAs in living cells. *J Biol Chem* 285, 17442-17452
14. Zhou, X., Lu, Z., Wang, T. et al. (2018) Plasma miRNAs in diagnosis and prognosis of pancreatic cancer: A miRNA expression analysis. *Gene* 673, 181-193
15. Xu, J., Cao, Z., Liu, W. et al. (2016) Plasma miRNAs Effectively Distinguish Patients With Pancreatic Cancer From Controls: A Multicenter Study. *Ann Surg* 263, 1173-1179
16. Cao, Z., Liu, C., Xu, J. et al. (2016) Plasma microRNA panels to diagnose pancreatic cancer: Results from a multicenter study. *Oncotarget* 7, 41575-41583
17. Miyamae, M., Komatsu, S., Ichikawa, D. et al. (2015) Plasma microRNA profiles: identification of miR-744 as a novel diagnostic and prognostic biomarker in pancreatic cancer. *Br J Cancer* 113, 1467-1476
18. Ganepola, G. A., Rutledge, J. R., Suman, P. et al. (2014) Novel blood-based microRNA biomarker panel for early diagnosis of pancreatic cancer. *World J Gastrointest Oncol* 6, 22-33
19. Kawaguchi, T., Komatsu, S., Ichikawa, D. et al. (2016) Circulating MicroRNAs: A Next-Generation Clinical Biomarker for Digestive System Cancers. *Int J Mol Sci* 17
20. Schwarzenbach, H., Nishida, N., Calin, G. A. et al. (2014) Clinical relevance of circulating cell-free microRNAs in cancer. *Nat Rev Clin Oncol* 11, 145-156

21. Shivapurkar, N., Vietsch, E. E., Carney, E. et al. (2017) Circulating microRNAs in patients with hormone receptor-positive, metastatic breast cancer treated with dovitinib. *Clin Transl Med* 6, 37
22. Rapisuwon, S., Vietsch, E. E. & Wellstein, A. (2016) Circulating biomarkers to monitor cancer progression and treatment. *Comput Struct Biotechnol J* 14, 211-222
23. Hingorani, S. R., Wang, L., Multani, A. S. et al. (2005) Trp53R172H and KrasG12D cooperate to promote chromosomal instability and widely metastatic pancreatic ductal adenocarcinoma in mice. *Cancer Cell* 7, 469-483
24. Mestdagh, P., Van Vlierberghe, P., De Weer, A. et al. (2009) A novel and universal method for microRNA RT-qPCR data normalization. *Genome Biol* 10, R64
25. Wan, G., Lim, Q. E. & Too, H. P. (2010) High-performance quantification of mature microRNAs by real-time RT-PCR using deoxyuridine-incorporated oligonucleotides and hemi-nested primers. *Rna* 16, 1436-1445
26. Groot, V. P., Daamen, L. A., Hagendoorn, J. et al. (2017) Current Strategies for Detection and Treatment of Recurrence of Pancreatic Ductal Adenocarcinoma After Resection: A Nationwide Survey. *Pancreas* 46, e73-e75
27. Wei, L., Yao, K., Gan, S. et al. (2018) Clinical utilization of serum- or plasma-based miRNAs as early detection biomarkers for pancreatic cancer: A meta-analysis up to now. *Medicine* (Baltimore) 97, e12132
28. Stroese, A. J., Ullerich, H., Koehler, G. et al. (2018) Circulating microRNA-99 family as liquid biopsy marker in pancreatic adenocarcinoma. *J Cancer Res Clin Oncol* Sep 17
29. Jarry, J., Schadendorf, D., Greenwood, C. et al. (2014) The validity of circulating microRNAs in oncology: five years of challenges and contradictions. *Mol Oncol* 8, 819-829
30. Pecqueux, M., Liebetrau, I., Werft, W. et al. (2016) A Comprehensive MicroRNA Expression Profile of Liver and Lung Metastases of Colorectal Cancer with Their Corresponding Host Tissue and Its Prognostic Impact on Survival. *Int J Mol Sci* 17
31. Pritchard, C. C., Kroh, E., Wood, B. et al. (2012) Blood cell origin of circulating microRNAs: a cautionary note for cancer biomarker studies. *Cancer Prev Res (Phila)* 5, 492-497
32. Williams, Z., Ben-Dov, I. Z., Elias, R. et al. (2013) Comprehensive profiling of circulating microRNA via small RNA sequencing of cDNA libraries reveals biomarker potential and limitations. *Proc Natl Acad Sci U S A* 110, 4255-4260
33. Aziz, M. H., Sideras, K., Aziz, N. A. et al. (2018) The Systemic-Immune-Inflammation Index Independently Predicts Survival and Recurrence in Resectable Pancreatic Cancer and its Prognostic Value Depends on Bilirubin Levels: A Retrospective Multicenter Cohort Study. *Ann Surg* Jan 12
34. Malumbres, R., Sarosiek, K. A., Cubedo, E. et al. (2009) Differentiation stage-specific expression of microRNAs in B lymphocytes and diffuse large B-cell lymphomas. *Blood* 113, 3754-3764
35. Bousquet, M., Harris, M. H., Zhou, B. et al. (2010) MicroRNA miR-125b causes leukemia. *Proc Natl Acad Sci U S A* 107, 21558-21563
36. Ooi, A. G., Sahoo, D., Adorno, M. et al. (2010) MicroRNA-125b expands hematopoietic stem cells and enriches for the lymphoid-balanced and lymphoid-biased subsets. *Proc Natl Acad Sci U S A* 107, 21505-21510
37. Liu, Q., Niu, Z., Li, Y. et al. (2016) Immunoglobulin G4 (IgG4)-positive plasma cell infiltration is associated with the clinicopathologic traits and prognosis of pancreatic cancer after curative resection. *Cancer Immunol Immunother* 65, 931-940
38. Huang, X., Yuan, T., Tschannen, M. et al. (2013) Characterization of human plasma-derived exosomal RNAs by deep sequencing. *BMC Genomics* 14, 319

39. Okoye, I. S., Coomes, S. M., Pelly, V. S. et al. (2014) MicroRNA-containing T-regulatory-cell-derived exosomes suppress pathogenic T helper 1 cells. *Immunity* 41, 89-103
40. Mittelbrunn, M., Gutierrez-Vazquez, C., Villarroya-Beltri, C. et al. (2011) Unidirectional transfer of microRNA-loaded exosomes from T cells to antigen-presenting cells. *Nat Commun* 2, 282
41. Nosirov, B., Billaud, J., Vandenbon, A. et al. (2017) Mapping circulating serum miRNAs to their immune-related target mRNAs. *Adv Appl Bioinform Chem* 10, 1-9
42. Zhu, Y., Zhang, S., Li, Z. et al. (2018) miR-125b-5p and miR-99a-5p downregulate human gammadelta T-cell activation and cytotoxicity. *Cell Mol Immunol* 2, 12
43. Li, Z., Jiang, C., Ye, C. et al. (2018) miR-10a-5p, miR-99a-5p and miR-21-5p are steroid-responsive circulating microRNAs. *Am J Transl Res* 10, 1490-1497
44. Tsai, T. F., Lin, J. F., Chou, K. Y. et al. (2018) miR-99a-5p acts as tumor suppressor via targeting to mTOR and enhances RAD001-induced apoptosis in human urinary bladder urothelial carcinoma cells. *Onco Targets Ther* 11, 239-252
45. Zhang, C., Zhang, C. D., Ma, M. H. et al. (2018) Three-microRNA signature identified by bioinformatics analysis predicts prognosis of gastric cancer patients. *World J Gastroenterol* 24, 1206-1215
46. Liu, Y., Zhang, D. T. & Liu, X. G. (2015) mTOR signaling in T cell immunity and autoimmunity. *Int Rev Immunol* 34, 50-66
47. Malik, N., Sansom, O. J. & Michie, A. M. (2018) The role of mTOR-mediated signals during haemopoiesis and lineage commitment. *Biochem Soc Trans* 8, 28
48. Karmaus, P. W. F., Herrada, A. A., Guy, C. et al. (2017) Critical roles of mTORC1 signaling and metabolic reprogramming for M-CSF-mediated myelopoiesis. *J Exp Med* 214, 2629-2647
49. Ward, J., Kanchagar, C., Veksler-Lublinsky, I. et al. (2014) Circulating microRNA profiles in human patients with acetaminophen hepatotoxicity or ischemic hepatitis. *Proc Natl Acad Sci U S A* 111, 12169-12174
50. Jopling, C. (2012) Liver-specific microRNA-122: Biogenesis and function. *RNA Biol* 9, 137-142
51. Ludwig, N., Leidinger, P., Becker, K. et al. (2016) Distribution of miRNA expression across human tissues. *Nucleic Acids Res* 44, 3865-3877
52. Versteijne, E., Vogel, J. A., Besselink, M. G. et al. (2018) Meta-analysis comparing upfront surgery with neoadjuvant treatment in patients with resectable or borderline resectable pancreatic cancer. *Br J Surg* 105, 946-958
53. Jang, J. Y., Han, Y., Lee, H. et al. (2018) Oncological Benefits of Neoadjuvant Chemoradiation With Gemcitabine Versus Upfront Surgery in Patients With Borderline Resectable Pancreatic Cancer: A Prospective, Randomized, Open-label, Multicenter Phase 2/3 Trial. *Ann Surg* 268, 215-222
54. Liu, Q., Liao, Q. & Zhao, Y. (2017) Chemotherapy and tumor microenvironment of pancreatic cancer. *Cancer Cell Int* 17, 68
55. Plate, J. M., Plate, A. E., Shott, S. et al. (2005) Effect of gemcitabine on immune cells in subjects with adenocarcinoma of the pancreas. *Cancer Immunol Immunother* 54, 915-925